

# Specific Heat and Thermal Diffusivity of Vinylidene Fluoride/Trifluoroethylene Copolymers

Y. W. Wong, N. M. Hui, E. L. Ong, H. L. W. Chan, C. L. Choy

Department of Applied Physics and Materials Research Centre, Hong Kong Polytechnic University, Hung Hom, Kowloon, Hong Kong

Received 26 November 2001; accepted 11 January 2003

**ABSTRACT:** The specific heat ( $C$ ) and thermal diffusivity ( $D$ ) of vinylidene fluoride (VDF)/trifluoroethylene copolymers with 70 and 56 mol % of VDF were measured between 200 and 390 K, and the thermal conductivity ( $K$ ) was calculated from these data.  $C$ ,  $D$ , and  $K$  were rather insensitive to the VDF content but varied significantly with the crystallinity. At room temperature, as the crystallinity increased from about 55 to 85%,  $C$  decreased by 17%, and  $D$  and  $K$  increased by 60 and 40%, respectively. For the copolymer with 70 mol

% VDF,  $C$  exhibited a broad peak, whereas  $D$  showed an abrupt drop at the ferroelectric–paraelectric transition near 370 K on heating. The transition temperature on cooling was about 40 K below that observed in the heating run, thus revealing a large thermal hysteresis. For the copolymer with 56 mol % VDF, the transition temperature was much lower, the transition region was narrower, and the thermal hysteresis was barely observable. © 2003 Wiley Periodicals, Inc. *J Appl Polym Sci* 89: 3160–3166, 2003

## INTRODUCTION

A strong piezoelectricity was observed by Kawai<sup>1</sup> in uniaxially drawn and poled films of polyvinylidene fluoride (PVDF) in 1969. Subsequently, pyroelectricity was also observed in such films.<sup>2</sup> PVDF is a semicrystalline polymer with a crystallinity ( $X$ ) of about 50%, and its crystallites can exist in one of the four polymorphic phases, designated as the  $\alpha$ ,  $\beta$ ,  $\gamma$ , and  $\delta$  phases. When PVDF is cooled from the melt, it crystallizes into an  $\alpha$  phase, which can be transformed by drawing below 370 K to a  $\beta$  phase with an all-trans conformation.<sup>3</sup> The dipoles of the molecular chains in the  $\beta$  phase are perpendicular to the chain direction, and the application of a suitable electric field to a drawn sample (i.e., poling) induces the dipoles to align in the direction of the field, thereby giving rise to a remnant polarization and, hence, piezoelectric and pyroelectric activities. Although a Curie transition point was not observed, other evidence, including the observation of polarization–electric field hysteresis loops,<sup>4</sup> has indicated that PVDF is a ferroelectric polymer.

Vinylidene fluoride (VDF)/trifluoroethylene (TrFE) copolymers [P(VDF/TrFE)'s] were synthesized in 1979, and soon afterward, the existence of a Curie transition point was established for copolymers with

VDF contents between 50 and 82 mol %.<sup>5,6</sup> The advantage of the copolymers over PVDF, as far as technical applications are concerned, is that the copolymers crystallize directly from the solution or melt into the  $\beta$  phase. Therefore, a drawing procedure, which is inconvenient in some applications, is not required to give piezoelectric and pyroelectric activities.

The piezoelectric and pyroelectric properties of PVDF and P(VDF/TrFE)'s have been exploited in various applications, including ultrasonic transducers and pyroelectric IR sensors and arrays. In pyroelectric sensor applications, thermal parameters such as specific heat ( $C$ ) and thermal diffusivity ( $D$ ) are required for the evaluation of the performance of the devices. The figures of merit for current responsivity, voltage responsivity, and detectivity of a pyroelectric sensor are inversely proportional to  $C$ .<sup>7</sup> Moreover, in the commonly used design of a copolymer film spin-coated on a silicon wafer containing a read-out circuit, the current and voltage responsivity can be calculated by the solution of the one-dimensional thermal diffusion equation for a multilayered system if  $C$  and  $D$  are known.<sup>8,9</sup> Finally, the thermal crosstalk between sensor elements in an array is determined by the thermal conductivity ( $K$ ) of the copolymer and is small if  $K$  is low.<sup>10</sup>

We previously studied  $C$ ,<sup>11</sup>  $D$ ,<sup>12,13</sup> and  $K$ <sup>14</sup> of PVDF. There have been some reports on  $C$  of P(VDF/TrFE)'s,<sup>15,16</sup> but almost no work has been done on  $D$  or  $K$ . In this work,  $C$  and  $D$  of P(VDF/TrFE)'s with 70 and 56 mol % of VDF were measured from 200 to 390 K, and  $K$  was calculated from these data. In particular, the effect of  $X$  and the behavior of  $C$  and  $D$  in the Curie transition region were studied in detail.

Correspondence to: Y. W. Wong (apaywwon@polyu.edu.hk).

Contract grant sponsor: Centre for Smart Materials.

Contract grant sponsor: Hong Kong Polytechnic University; contract grant number: G-V409.

TABLE I  
Physical Properties of P(VDF/TrFE) 70/30

	X	$\rho$ (g/cm <sup>3</sup> )	C (J/g K)	D ( $\times 10^{-3}$ cm <sup>2</sup> /s)	K (mW/cm K)
Slow-cooled					
200 K	—	1.953	0.692	1.57	2.12
295 K	0.80	1.917	1.04	1.09	2.18
Quenched					
200 K	—	1.920	0.690	1.18	1.56
295 K	0.55	1.886	1.19	0.745	1.67

## EXPERIMENTAL

### Sample preparation

P(VDF/TrFE)'s with 70 mol % VDF [denoted as P(VDF/TrFE) 70/30] and 56 mol % VDF [denoted as P(VDF/TrFE) 56/44] were supplied in pellet form by Piezotech (Saint-Louis, France). The pellets were compression-molded at 190°C into sheets about 0.2 mm in thickness. The sheets were either slowly cooled at a rate of 0.5 K/min or quenched in iced water. We prepared another series of samples by annealing the quenched sheets at various temperatures from 373 to 413 K.

### X, density ( $\rho$ ), and C measurements

X-ray diffraction measurements were performed on the copolymer samples in the  $2\theta$  range 10–30°. The X-ray profiles revealed a sharp peak near  $2\theta = 20^\circ$  associated with the (110) and (200) reflections of the crystallites and a broad shoulder on its low-angle side associated with the halo contributed by the amorphous regions.<sup>17</sup> We separated the crystalline peak and the amorphous halo by fitting each of them to a Gaussian function. Then, we evaluated X by dividing the area under the crystalline peak by the total area under the two peaks.

$\rho$  of the samples at room temperature was measured by the flotation method. To find the temperature dependence of  $\rho$ , the dimensional change of the slow-cooled and quenched samples was determined in a heating-cooling cycle between 200 and 390 K with a PerkinElmer TMA-7 thermomechanical analyzer. The dimension change was also used to convert the ob-

served sample thickness at room temperature to the actual thickness at any given temperature, which was required for the calculation of  $D$  from the raw data.

C of the samples was measured with an accuracy of 3% by a PerkinElmer DSC-7 differential scanning calorimeter at a rate of 10 K/min. Measurements were performed in a heating-cooling cycle between 200 and 390 K.

### D measurements

The technique for the measurement of  $D$  by the laser flash method was discussed in detail in a previous publication.<sup>13</sup> Briefly, a sample about 8 mm in diameter and 0.2 mm in thickness was clamped on its edge to a copper sample holder placed in an evacuated chamber. The sample was controlled at a given temperature ( $T$ ) and a laser beam of wavelength 532 nm and diameter 4 mm was flashed from a pulsed Nd/YAG laser to the front surface of the sample. A thin carbon layer was coated on this surface to enhance the absorption of the laser beam.

The thermal radiation from the back surface was focused by a germanium lens onto a liquid-nitrogen-cooled HgCdTe detector. The amplified signal was measured as a function of time with a Hewlett-Packard 54510 digitizing oscilloscope. Depending on the signal magnitude, we performed the experiment by averaging the results for 30–80 laser shots. A microcomputer was used to collect the data and fit them to a theoretical expression<sup>13</sup> to give  $D(T)$ . The estimated accuracy of the measurement was 3%.  $K(T)$ , calculated from  $K = \rho CD$ , thus, the measurement had an accuracy of 6%.

TABLE II  
Physical Properties of P(VDF/TrFE) 56/44

	X	$\rho$ (g/cm <sup>3</sup> )	C (J/g K)	D ( $\times 10^{-3}$ cm <sup>2</sup> /s)	K (mW/cm K)
Slow-cooled					
200 K	—	1.952	0.665	1.56	2.03
295 K	0.65	1.906	1.06	1.06	2.13
Quenched					
200 K	—	1.934	0.680	1.16	1.53
295 K	0.45	1.885	1.20	0.730	1.64

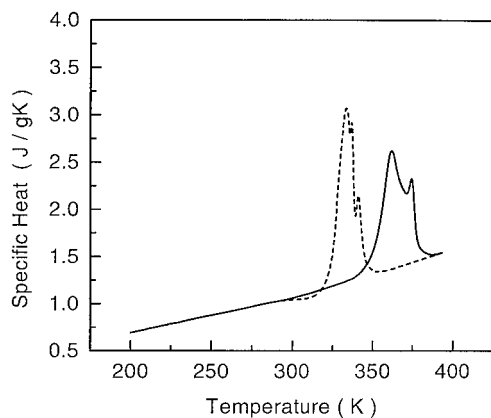


**Figure 1**  $C$  of slow-cooled P(VDF/TrFE) 70/30 as a function of temperature: data obtained in (—) heating and (---) cooling runs.

## RESULTS AND DISCUSSION

$C$  and  $D$  of the quenched and slow-cooled samples of P(VDF/TrFE) with 70 and 56 mol % VDF were measured from 200 to 390 K, and  $K$  was calculated from these data. Tables I and II show the data at 200 and 295 K for P(VDF/TrFE) 70/30 and P(VDF/TrFE) 56/44, respectively.  $C$ ,  $D$ , and  $K$  depended weakly on the VDF content but more significantly on  $X$ . Below the glass-transition temperature ( $T_g$ ;  $T_g \approx 240$  K),<sup>18</sup>  $C$  was roughly independent of  $X$ . Above  $T_g$ , however,  $C$  of the quenched samples [ $X = 0.45$ – $0.55$ ] became increasingly higher than that of the slow-cooled samples ( $X = 0.65$ – $0.8$ ), and the difference reached about 13% at 295 K. Because the quenched sample had a higher amorphous content than the slow-cooled sample, the micro-Brownian motion of the chains in the amorphous regions gave rise to a higher contribution to  $C$ . Tables I and II also show that both  $D$  and  $K$  increased with  $X$ , which implies that  $D$  and the conductivity of the anisotropic crystallites, averaged over all directions, were higher than those of the amorphous ma-

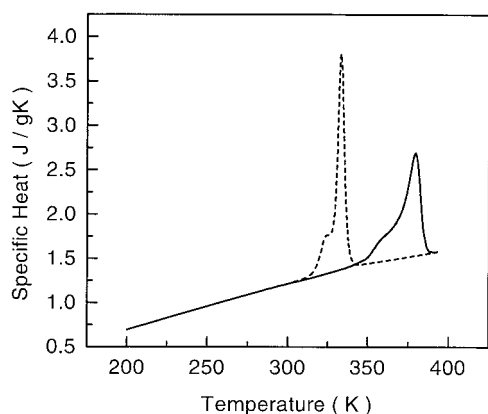


**Figure 2**  $C$  of quenched P(VDF/TrFE) 70/30 as a function of temperature: data obtained in (—) heating and (---) cooling runs.

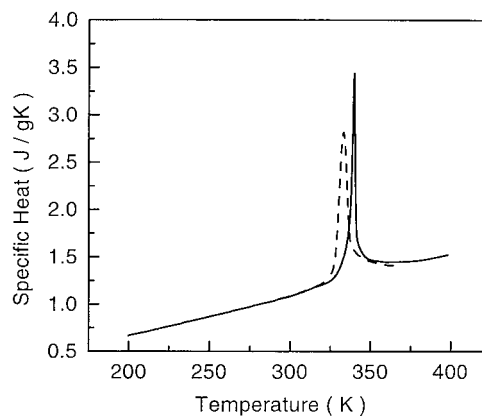


**Figure 3**  $C$  of slow-cooled P(VDF/TrFE) 56/44 as a function of temperature: data obtained in (—) heating and (---) cooling runs.

trix. This behavior is generally observed in semicrystalline polymers.<sup>12–14</sup>

## $C$

Figures 1 and 2 show  $C$ s of slow-cooled and quenched P(VDF/TrFE) with 70 mol % VDF, respectively. A broad peak occurred at the ferroelectric–paraelectric transition (Curie transition), at which the all-trans conformation of the chains in the crystallites changes into a random mixture of TG+, TG–, TTTG– sequences.<sup>3</sup> The peak observed in the cooling run appeared at about 40 K lower than that observed in the heating run. The large thermal hysteresis was observed previously by various workers.<sup>15,19–21</sup>

Figures 1 and 2 also show that the broad peak was composed of two or three narrower peaks. It was suggested<sup>22</sup> that these narrow peaks correspond to the ferroelectric–paraelectric transitions in crystallites with different degrees of perfection, with the peak at the highest temperature associated with the most per-

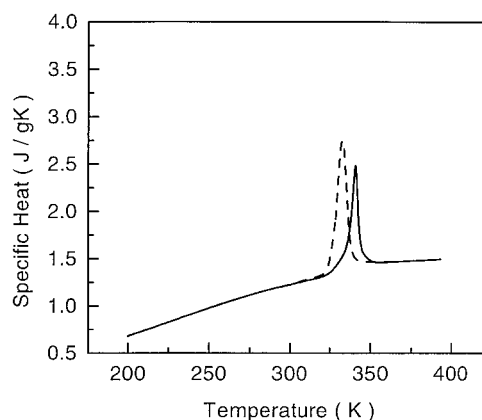


**Figure 4**  $C$  of quenched P(VDF/TrFE) 56/44 as a function of temperature: data obtained in (—) heating and (---) cooling runs.

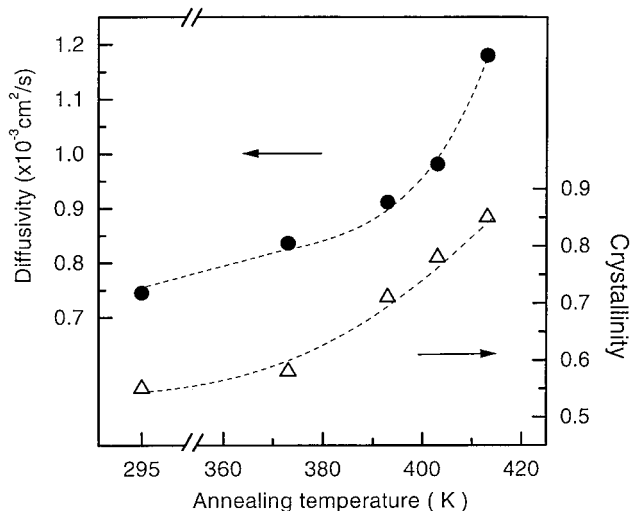


**Figure 5** *D* and *X* of quenched P(VDF/TrFE) 70/30 as a function of annealing temperature.

fect crystallites. The imperfection may be strain-induced or may arise from conformational defects.

Figures 3 and 4 show *C<sub>s</sub>* of slow-cooled and quenched P(VDF/TrFE) with 56 mol % VDF, respectively. Comparing these figures with Figures 1 and 2, we observed that the VDF content decreased from 70 to 56 mol %, the transition occurred at a much lower temperature, the transition peak became narrower, and the thermal hysteresis became much smaller.

**D**

As shown in Table I, because of the higher *X*, the slow-cooled sample had a room-temperature *D* that was about 45% higher than that of the quenched sample. To investigate *X* effect in more detail, we annealed

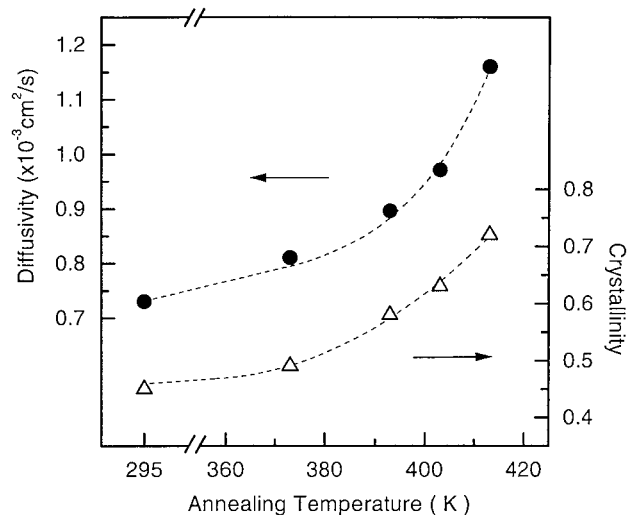


**Figure 6** *D* and *X* of quenched P(VDF/TrFE) 56/44 as a function of annealing temperature.

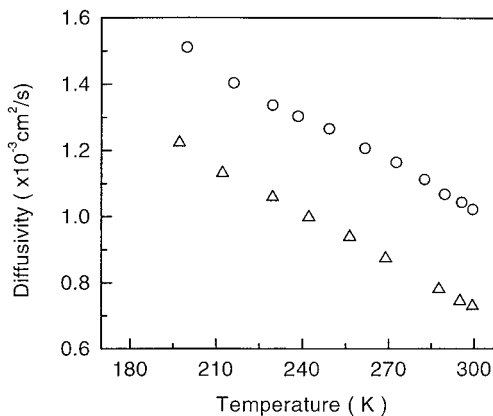


**Figure 7** *D* of P(VDF/TrFE) 70/30 as a function of temperature: (○) slow-cooled sample and (△) quenched sample.

quenched samples of the two copolymers for 2 h at various temperatures up to 413 K; then, *D* was measured at room temperature. As shown in Figures 5 and 6, both *X* and *D* increased only slightly at annealing temperatures below 373 K, but they increased much more rapidly at higher annealing temperatures. After annealing at 413 K, the crystallinities of P(VDF/TrFE) 70/30 and P(VDF/TrFE) 56/44 reached high values of 0.85 and 0.72, respectively, and the *D*s of both copolymers were about  $1.17 \times 10^{-3} \text{ cm}^2 \text{ s}^{-1}$ , that is, 60% higher than those of the quenched samples. The slow-cooled samples had *X* and *D* values similar to those of samples annealed at 405 K. This was reasonable because the copolymers crystallized rapidly near this temperature, as revealed by the occurrence of a crystallization peak during cooling runs.<sup>21</sup> Figure 7 shows *D*s of slow-cooled and quenched P(VDF/TrFE) 70/30 below room temperature. *D*s of the slow-cooled and quenched samples exhibited similar temperature dependencies and decreased significantly with increasing temperature. The temperature dependence of *D* for slow-cooled P(VDF/TrFE) 70/30 above room tem-

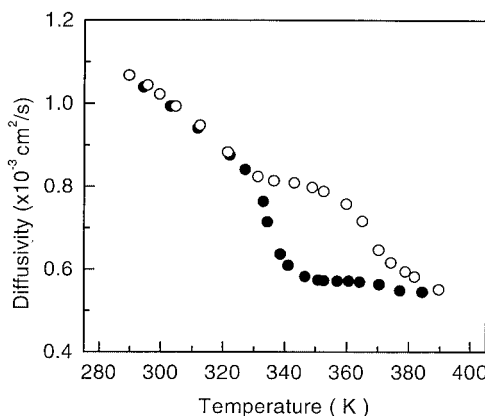


**Figure 8** *D* of slow-cooled P(VDF/TrFE) 70/30 as a function of temperature: data obtained in (○) heating and (●) cooling runs.

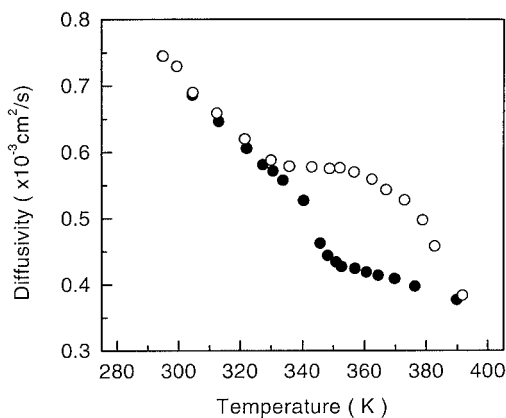


**Figure 9**  $D$  of quenched P(VDF/TrFE) 70/30 as a function temperature: data obtained in (○) heating and (●) cooling runs.

perature is shown in Figure 8. An abrupt drop in  $D$  was observed at the Curie transition temperature ( $T_c$ ;  $T_c \approx 370$  K) on heating. In the cooling run, however, the sudden change occurred at about 332 K, giving a shift in the transition temperature of about 38 K. A similar change in the sound velocity was also observed in Brillouin scattering<sup>23,24</sup> and ultrasonic<sup>25</sup> experiments. As shown in Figure 9, the quenched sample exhibited the same features as the slow-cooled sample, but the value of  $D$  was lower over the entire temperature range. The highest temperature reached in the heating run was about 390 K. However, because the dwelling time at such a high temperature was only 10 min, there was very little change in  $X$ ,  $C$  (see Figs. 1 and 2), and  $D$  (see Figs. 9 and 10) after the heating-cooling cycle.

The temperature dependence of  $D$  for P(VDF/TrFE) 56/44 below room temperature is shown in Figure 10, whereas those for slow-cooled and quenched P(VDF/TrFE) 56/44 above room temperature are shown in Figures 11 and 12, respectively. Again, abrupt changes in  $D$  were observed at the Curie transition. However,

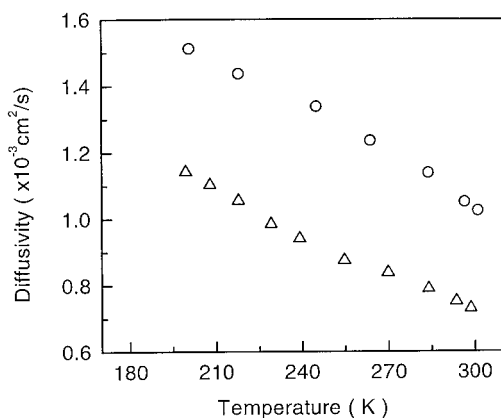


**Figure 10**  $D$  of P(VDF/TrFE) 56/44 as a function of temperature: (○) slow-cooled sample and (△) quenched sample.

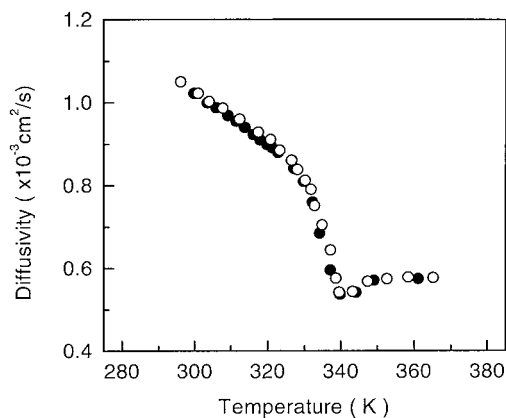


**Figure 11**  $D$  of slow-cooled P(VDF/TrFE) 56/44 as a function of temperature: data obtained in (○) heating and (●) cooling runs.

the thermal hysteresis was so small that it was barely observable. The high-temperature limit of the heating run was 367 K, and there were no observable changes in  $X$ ,  $C$ , and  $D$  after the heating-cooling cycle.

## $K$

Figures 13 and 14 show the temperature dependence of  $K$  ( $= \rho CD$ ) for slow-cooled and quenched P(VDF/TrFE) 70/30, respectively. At 200 K,  $K$  of the slow-cooled sample ( $X = 0.8$ ) had a value of 2.1 mW/cm K. It increased slightly with temperature, reached a shallow maximum near  $T_g$  ( $\sim 240$  K), and then decreased. Previously, we studied  $K$  of various semicrystalline polymers as a function of temperature<sup>12-14,26</sup> and developed a two-phase model<sup>27</sup> to explain its behavior. The model predicts that  $K$  depends on  $X$ , the thermal conductivity of the amorphous matrix ( $K_a$ ), and the thermal conductivity of the crystallites normal to the chain axis ( $K_{c\perp}$ ).  $K$  does not depend on the thermal conductivity of the crystallites parallel to the chain

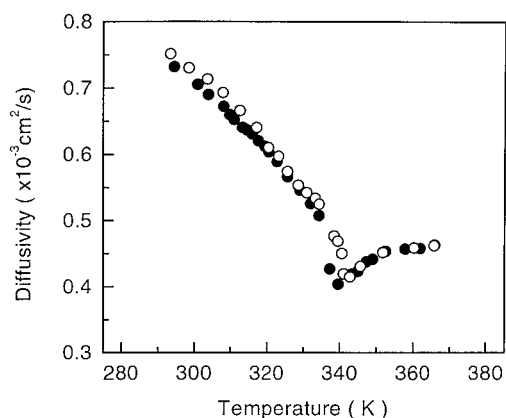


**Figure 12**  $D$  of quenched P(VDF/TrFE) 56/44 as a function of temperature: data obtained in (○) heating and (●) cooling runs.

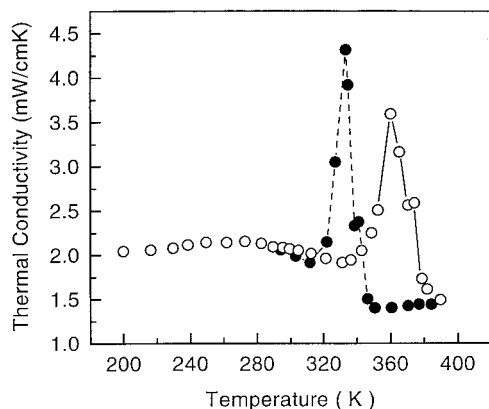


**Figure 13**  $K$  of slow-cooled P(VDF/TrFE) 70/30 as a function of temperature: data obtained in (○) heating and (●) cooling runs.

axis ( $K_{c||}$ ) because  $K_{c||}$  is so much larger than  $K_a$  that its effect has been saturated.  $K_a$  is generally low and has a weak positive temperature dependence between 100 and 300 K. Thus, the low value and weak temperature dependence of  $K$  of slow-cooled P(VDF/TrFE) 70/30 reflected the behavior of  $K_{c\perp}$ . As discussed previously,<sup>12</sup> a low magnitude and weak temperature dependence for  $K_{c\perp}$  implies that the crystallites had a significant number of defects.

As the slow-cooled sample was heated further,  $K$  rose sharply to a peak value at  $T_c$  and then dropped to a value that was about 35% lower than just below the transition. The peak and the subsequent drop reflected the behavior of  $C$  and  $D$ , respectively, because the 5% drop in  $\rho$  at the transition made only a minor contribution.  $K$  of the quenched sample exhibited a similar temperature dependence but its magnitude was about 30% lower.

Figures 15 and 16 show that the slow-cooled and quenched samples of P(VDF/TrFE) 56/44 exhibited similar features, except that the Curie transition on

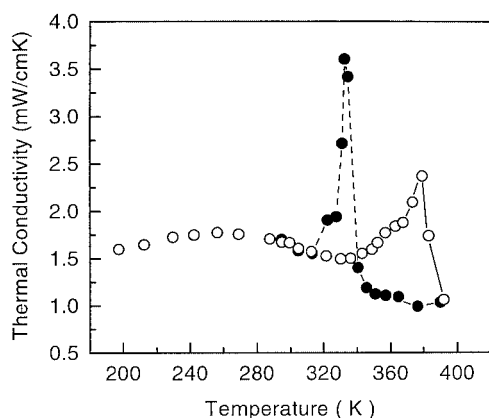


**Figure 14**  $K$  of quenched P(VDF/TrFE) 70/30 as a function of temperature: data obtained in (○) heating and (●) cooling runs.

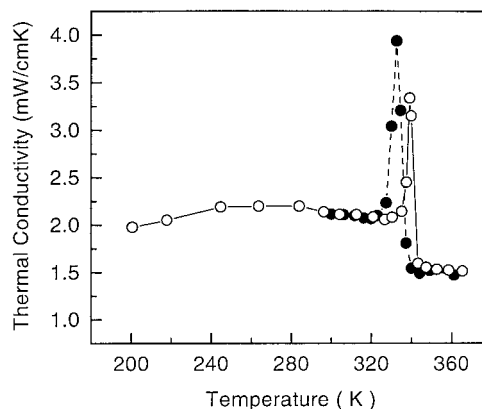


**Figure 15**  $K$  of slow-cooled P(VDF/TrFE) 56/44 as a function of temperature: data obtained in (○) heating and (●) cooling runs.

heating occurred at a much lower temperature, the transition region was narrower, and the thermal hysteresis was much smaller.

## CONCLUSIONS

$C$ ,  $D$ , and  $K$  of P(VDF/TrFE) depended weakly on the VDF content but more significantly on  $X$ . At room temperature, as  $X$  increased from about 55 to 85%,  $C$  decreased by almost 17%, whereas  $D$  and  $K$  increased by about 60 and 40%, respectively. The decrease in  $C$  was due to the reduced contribution of the mobile chains in the amorphous regions as a result of the decrease in amorphous content. The increases in  $D$  and  $K$  reflected the fact that, like other semicrystalline polymers,<sup>12-14,26,27</sup> the crystallites of P(VDF/TrFE) had higher  $D$  and conductivity than the amorphous regions. Compared with  $K$  of polyethylene at the same  $X$ ,  $K$  of P(VDF/TrFE) had a much lower magnitude and a weaker temperature dependence, thus indicat-

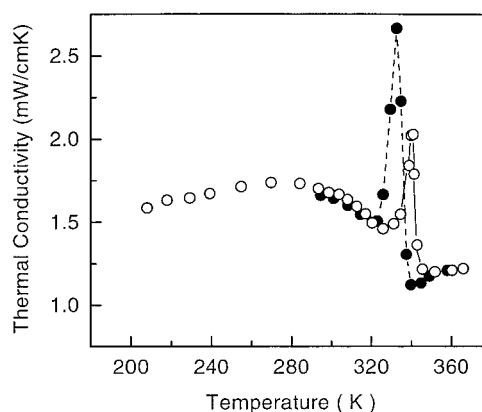


**Figure 16**  $K$  of quenched P(VDF/TrFE) 56/44 as a function of temperature: data obtained in (○) heating and (●) cooling runs.

ing that there were a significant number of defects in the crystallites.

*C* exhibited two to three peaks in the ferroelectric–paraelectric transition region. At a VDF content of 70 mol %, there was a large thermal hysteresis in which the transition on cooling appeared at about 40 K lower than that observed in the heating run. As the VDF content decreased to 56 mol %, the difference in  $T_c$  observed in heating and cooling runs decreased to about 6 K.

On heating, *D* showed an abrupt drop at  $T_c$ . Like *C*, a thermal hysteresis was observed. As the VDF content decreased from 70 to 56 mol %,  $T_c$  decreased drastically, the transition region became narrower, and the thermal hysteresis became very small. The behavior of *K* at the transition simply reflected that of *C* and *D*. Therefore, *K* exhibited a peak at  $T_c$  followed by a drop.

## References

1. Kawai, H. *Jpn J Appl Phys* 1969, 8, 875.
2. Bergman, J. G.; McFee, J. H.; Crane, G. R. *Appl Phys Lett* 1971, 18, 203.
3. Tashiro, K. In *Ferroelectric Polymers*; Nalwa, H. R., Ed.; Marcel Dekker: New York, 1995; p 63.
4. Furukawa, T.; Date, M.; Fukada, E. *J Appl Phys* 1980, 51, 1135.
5. Yagi, T.; Tatamoto, M.; Sako, J. I. *Polym J* 1980, 12, 209.
6. Furukawa, T.; Date, M.; Fukada, E.; Tajitsu, Y.; Chiba, A. *Jpn J Appl Phys* 1980, 19, L109.
7. Whatmore, R. W. *Ferroelectrics* 1991, 118, 241.
8. Lienhard, D.; Ploss, B. *J Appl Phys* 1995, 77, 5426.
9. Chen, Y.; Chan, H. L. W.; Hui, N. M.; Wong, Y. W.; Choy, C. L. *Sens Actuators A* 1998, 69, 156.
10. Köhler, R.; Neumann, N.; Gottfried-Gottfried, R. *Microelectron Eng* 1995, 29, 79.
11. Lee, W. K.; Choy, C. L. *J Polym Sci Polym Phys Ed* 1975, 13, 619.
12. Choy, C. L.; Ong, E. L.; Chen, F. C. *J Appl Polym Sci* 1981, 26, 2325.
13. Choy, C. L.; Leung, W. P.; Ng, Y. K. *J Polym Sci Part B: Polym Phys* 1987, 25, 1779.
14. Choy, C. L.; Chen, F. C.; Luk, W. H. *J Polym Sci Polym Phys Ed* 1980, 18, 1187.
15. Furukawa, T.; Johnson, G. E.; Bair, H. E.; Tajitsu, Y.; Chiba, A.; Fukada, E. *Ferroelectrics* 1981, 32, 61.
16. Li, G. R.; Ohigashi, H. *Jpn J Appl Phys* 1992, 31, 2495.
17. Ikeda, S.; Shimojima, Z.; Kutani, M. *Ferroelectrics* 1990, 109, 297.
18. Teyssedre, G.; Lacabanne, C. *Polymer* 1995, 36, 3641.
19. Furukawa, T.; Johnson, G. E. *J Appl Phys* 1981, 52, 940.
20. Tashiro, K.; Takano, K.; Kobayashi, M.; Chatani, Y.; Tadokoro, H. *Ferroelectrics* 1984, 57, 297.
21. Koga, K.; Ohigashi, H. *J Appl Phys* 1986, 59, 2145.
22. Moreira, R. L.; Saint-Gregoire, P.; Lopez, M.; Latour, M. *J Polym Sci Part B: Polym Phys* 1989, 27, 709.
23. Krüger, J. K.; Petzelt, J.; Legrand, J. F. *Colloid Polym Sci* 1986, 264, 791.
24. Krüger, J. K.; Prechtel, M.; Legrand, J. F. *Ferroelectrics* 1990, 109, 315.
25. Tashiro, K.; Itoh, Y.; Nishimura, S.; Kobayashi, M. *Polymer* 1991, 32, 1017.
26. Choy, C. L. *Polymer* 1977, 18, 984.
27. Choy, C. L.; Young, K. *Polymer* 1977, 18, 769.